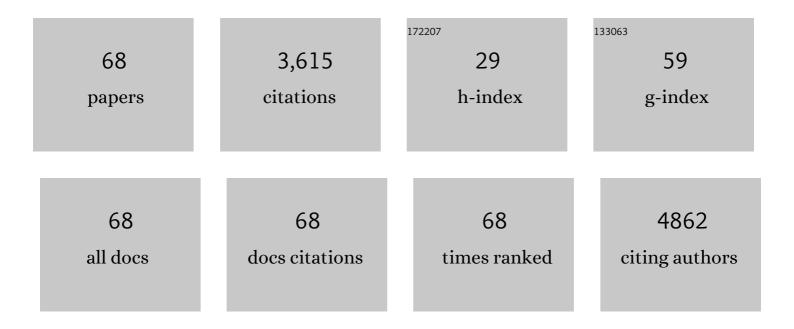
List of Publications by Year in descending order

Source: https://exaly.com/author-pdf/5811765/publications.pdf Version: 2024-02-01



SHENCCEN YAO

#	Article	IF	CITATIONS
1	NMR spectroscopy of lipidic cubic phases. Biophysical Reviews, 2022, 14, 67-74.	1.5	8
2	NMR measurement of biomolecular translational and rotational motion for evaluating changes of protein oligomeric state in solution. European Biophysics Journal, 2022, 51, 193-204.	1.2	3
3	Chemical Exchange of Hydroxyl Groups in Lipidic Cubic Phases Characterized by NMR. Journal of Physical Chemistry B, 2021, 125, 571-580.	1.2	5
4	Water diffusion in complex systems measured by PGSEÂNMR using chemical shift selective stimulated echo: Elimination of magnetization exchange effects. Journal of Chemical Physics, 2021, 155, 224203.	1.2	2
5	Physiochemical Characterization and Stability of Lipidic Cubic Phases by Solution NMR. Langmuir, 2020, 36, 6254-6260.	1.6	8
6	Heteronuclear NMR spectroscopy of proteins encapsulated in cubic phase lipids. Journal of Magnetic Resonance, 2019, 305, 146-151.	1.2	11
7	Structural insights into BCL2 pro-survival protein interactions with the key autophagy regulator BECN1 following phosphorylation by STK4/MST1. Autophagy, 2019, 15, 785-795.	4.3	38
8	The molecular basis of JAK/STAT inhibition by SOCS1. Nature Communications, 2018, 9, 1558.	5.8	298
9	Discovery and characterization of a sulfoquinovose mutarotase using kinetic analysis at equilibrium by exchange spectroscopy. Biochemical Journal, 2018, 475, 1371-1383.	1.7	18
10	Measuring translational diffusion of 15N-enriched biomolecules in complex solutions with a simplified 1H-15N HMQC-filtered BEST sequence. European Biophysics Journal, 2018, 47, 891-902.	1.2	9
11	Predicting the release profile of small molecules from within the ordered nanostructured lipidic bicontinuous cubic phase using translational diffusion coefficients determined by PFG-NMR. Nanoscale, 2017, 9, 2471-2478.	2.8	38
12	Lipidic Cubic Phase-Induced Membrane Protein Crystallization: Interplay Between Lipid Molecular Structure, Mesophase Structure and Properties, and Crystallogenesis. Crystal Growth and Design, 2017, 17, 5667-5674.	1.4	16
13	Câ€Terminal Modification and Multimerization Increase the Efficacy of a Prolineâ€Rich Antimicrobial Peptide. Chemistry - A European Journal, 2017, 23, 390-396.	1.7	28
14	The BECN1ÂN-terminal domain is intrinsically disordered. Autophagy, 2016, 12, 460-471.	4.3	21
15	Characterisation of the conformational preference and dynamics of the intrinsically disordered N-terminal region of Beclin 1 by NMR spectroscopy. Biochimica Et Biophysica Acta - Proteins and Proteomics, 2016, 1864, 1128-1137.	1.1	5
16	Characterization of the Lipid-Binding Site of Equinatoxin II by NMR and Molecular Dynamics Simulation. Biophysical Journal, 2015, 108, 1987-1996.	0.2	42
17	Nutation frequency modulation on NMR signal of nuclear spins in chemical exchange with solvent water under the BEST conditions. Magnetic Resonance in Chemistry, 2014, 52, 190-194.	1.1	2
18	NMR studies of interactions between Bax and BH3 domain-containing peptides in the absence and presence of CHAPS. Archives of Biochemistry and Biophysics, 2014, 545, 33-43.	1.4	11

#	Article	IF	CITATIONS
19	Measuring translational diffusion coefficients of peptides and proteins by PFG-NMR using band-selective RF pulses. European Biophysics Journal, 2014, 43, 331-339.	1.2	30
20	Hydrodynamic radii of solubilized high amylose native and modified starches by pulsed field gradient NMR diffusion measurements. Food Hydrocolloids, 2014, 40, 16-21.	5.6	5
21	Bax Crystal Structures Reveal How BH3 Domains Activate Bax and Nucleate Its Oligomerization to Induce Apoptosis. Cell, 2013, 152, 519-531.	13.5	491
22	Murine Interleukin-3: Structure, Dynamics, and Conformational Heterogeneity in Solution. Biochemistry, 2011, 50, 2464-2477.	1.2	18
23	Exchange enhanced sensitivity gain for solvent-exchangeable protons in 2D 1H–15N heteronuclear correlation spectra acquired with band-selective pulses. Journal of Magnetic Resonance, 2011, 211, 243-247.	1.2	13
24	Peptide inhibitors of the malaria surface protein, apical membrane antigen 1: Identification of key binding residues. Biopolymers, 2011, 95, 354-364.	1.2	12
25	1H, 13C and 15N resonance assignments of a highly-soluble murine interleukin-3 analogue with wild-type bioactivity. Biomolecular NMR Assignments, 2010, 4, 73-77.	0.4	6
26	The SPRY domain–containing SOCS box protein SPSB2 targets iNOS for proteasomal degradation. Journal of Cell Biology, 2010, 190, 129-141.	2.3	88
27	Structural Basis for Par-4 Recognition by the SPRY Domain- and SOCS Box-Containing Proteins SPSB1, SPSB2, and SPSB4. Journal of Molecular Biology, 2010, 401, 389-402.	2.0	63
28	The SPRY domain–containing SOCS box protein SPSB2 targets iNOS for proteasomal degradation. Journal of Experimental Medicine, 2010, 207, i22-i22.	4.2	0
29	Antibodies specifically targeting a locally misfolded region of tumor associated EGFR. Proceedings of the United States of America, 2009, 106, 5082-5087.	3.3	69
30	Insulin-like growth factor-I (IGF-I): Solution properties and NMR chemical shift assignments near physiological pH. Growth Hormone and IGF Research, 2009, 19, 226-231.	0.5	3
31	SPRY Domain-Containing SOCS Box Protein 2: Crystal Structure and Residues Critical for Protein Binding. Journal of Molecular Biology, 2009, 386, 662-674.	2.0	40
32	Coarseâ€grained dynamics of the receiver domain of NtrC: Fluctuations, correlations and implications for allosteric cooperativity. Proteins: Structure, Function and Bioinformatics, 2008, 73, 218-227.	1.5	11
33	Protein effective rotational correlation times from translational self-diffusion coefficients measured by PFG-NMR. Biophysical Chemistry, 2008, 136, 145-151.	1.5	36
34	Solution Conformation, Backbone Dynamics and Lipid Interactions of the Intrinsically Unstructured Malaria Surface Protein MSP2. Journal of Molecular Biology, 2008, 379, 105-121.	2.0	59
35	The SOCS Box Domain of SOCS3: Structure and Interaction with the ElonginBC-Cullin5 Ubiquitin Ligase. Journal of Molecular Biology, 2008, 381, 928-940.	2.0	91
36	Structure, Dynamics, and Selectivity of the Sodium Channel Blocker μ-Conotoxin SIIIA. Biochemistry, 2008, 47, 10940-10949.	1.2	65

#	Article	IF	CITATIONS
37	Cooperativity of the N- and C-Terminal Domains of Insulin-like Growth Factor (IGF) Binding Protein 2 in IGF Binding. Biochemistry, 2007, 46, 13720-13732.	1.2	26
38	The N-Terminal Subdomain of Insulin-like Growth Factor (IGF) Binding Protein 6. Structure and Interaction with IGFsâ€. Biochemistry, 2007, 46, 3065-3074.	1.2	20
39	Merozoite surface protein 2 ofPlasmodium falciparum: Expression, structure, dynamics, and fibril formation of the conserved N-terminal domain. Biopolymers, 2007, 87, 12-22.	1.2	43
40	Structure, Dynamics and Heparin Binding of the C-terminal Domain of Insulin-like Growth Factor-binding Protein-2 (IGFBP-2). Journal of Molecular Biology, 2006, 364, 690-704.	2.0	50
41	The Structure of SOCS3 Reveals the Basis of the Extended SH2 Domain Function and Identifies an Unstructured Insertion That Regulates Stability. Molecular Cell, 2006, 22, 205-216.	4.5	140
42	The SPRY domain of SSB-2 adopts a novel fold that presents conserved Par-4–binding residues. Nature Structural and Molecular Biology, 2006, 13, 77-84.	3.6	72
43	Dynamics of the SPRY domain-containing SOCS box protein 2: Flexibility of key functional loops. Protein Science, 2006, 15, 2761-2772.	3.1	14
44	Copper and Zinc Mediated Oligomerisation of AÎ <sup>2</sup> Peptides. International Journal of Peptide Research and Therapeutics, 2006, 12, 153-164.	0.9	35
45	Secondary structure assignment of mouse SOCS3 by NMR defines the domain boundaries and identifies an unstructured insertion in the SH2 domain. FEBS Journal, 2005, 272, 6120-6130.	2.2	45
46	Letter to the Editor: Backbone 1H, 13C and 15N assignments of the 25 kDa SPRY domain-containing SOCS box protein 2 (SSB-2). Journal of Biomolecular NMR, 2005, 31, 69-70.	1.6	14
47	Structure and Inter-domain Interactions of Domain II from the Blood-stage Malarial Protein, Apical Membrane Antigen 1. Journal of Molecular Biology, 2005, 350, 641-656.	2.0	30
48	Affinity Maturation of Leukemia Inhibitory Factor and Conversion to Potent Antagonists of Signaling. Journal of Biological Chemistry, 2004, 279, 2125-2134.	1.6	30
49	C-Terminal Domain of Insulin-Like Growth Factor (IGF) Binding Protein-6: Structure and Interaction with IGF-II. Molecular Endocrinology, 2004, 18, 2740-2750.	3.7	44
50	Characterizing bathocuproine self-association and subsequent binding to Alzheimer's disease amyloidβ-peptide by NMR. Journal of Peptide Science, 2004, 10, 210-217.	0.8	24
51	C-Terminal Domain of Insulin-like Growth Factor (IGF) Binding Protein 6:Â Conformational Exchange and Its Correlation with IGF-II Bindingâ€. Biochemistry, 2004, 43, 11187-11195.	1.2	16
52	Binding site for the C-domain of insulin-like growth factor (IGF) binding protein-6 on IGF-II; implications for inhibition of IGF actions. FEBS Letters, 2004, 568, 19-22.	1.3	21
53	1H, 13C and 15N resonance assignments of the C-terminal domain of insulin-like growth factor binding protein-6 (IGFBP-6). Journal of Biomolecular NMR, 2003, 25, 251-252.	1.6	5
54	Stabilization of the Helical Structure of Y2-Selective Analogues of Neuropeptide Y by Lactam Bridges. Journal of Medicinal Chemistry, 2002, 45, 2310-2318.	2.9	16

#	Article	IF	CITATIONS
55	Aromatase-deficient (ArKO) mice accumulate excess adipose tissue. Journal of Steroid Biochemistry and Molecular Biology, 2001, 79, 3-9.	1.2	117
56	Gradient refractive index of the crystalline lens of the Black Oreo Dory (Allocyttus Niger): comparison of magnetic resonance imaging (MRI) and laser ray-trace methods. Vision Research, 2001, 41, 973-979.	0.7	43
57	Peptide self-association in aqueous trifluoroethanol monitored by pulsed field gradient NMR diffusion measurements. Journal of Biomolecular NMR, 2000, 16, 109-119.	1.6	99
58	Aromatase-deficient (ArKO) mice have a phenotype of increased adiposity. Proceedings of the National Academy of Sciences of the United States of America, 2000, 97, 12735-12740.	3.3	650
59	Backbone dynamics measurements on leukemia inhibitory factor, a rigid fourâ€helical bundle cytokine. Protein Science, 2000, 9, 671-682.	3.1	13
60	Improved Estimation of Protein Rotational Correlation Times from15N Relaxation Measurements. Journal of Magnetic Resonance, 1998, 131, 347-350.	1.2	12
61	Solution structure of peptides from HIV-1 Vpr protein that cause membrane permeabilization and growth arrest. , 1998, 4, 426-435.		9
62	An investigation of concentration polarization phenomena in membrane filtration of colloidal silica suspensions by NMR micro-imaging. Journal of Membrane Science, 1998, 145, 145-158.	4.1	59
63	An investigation of the fluidity of concentration polarisation layers in crossflow membrane filtration of an oil-water emulsion using chemical shift selective flow imaging. Magnetic Resonance Imaging, 1997, 15, 235-242.	1.0	21
64	Quantitative measurements of the concentration polarisation layer thickness in membrane filtration of oil-water emulsions using NMR micro-imaging. Journal of Membrane Science, 1996, 118, 247-257.	4.1	50
65	Non-invasive observation of flow profiles and polarisation layers in hollow fibre membrane filtration modules using NMR micro-imaging. Journal of Membrane Science, 1995, 99, 207-216.	4.1	75
66	Quantitative magnetic resonance flow and diffusion imaging in porous media. Magnetic Resonance Imaging, 1995, 13, 729-738.	1.0	21
67	Quantitative NMR imaging of flow. Concepts in Magnetic Resonance, 1993, 5, 281-302.	1.3	120
68	Flow-selective pulse sequences. Magnetic Resonance Imaging, 1993, 11, 585-591.	1.0	18